New Journal of Physics
The open-access journal for physics

New J. Phys. **11** (2009) 013015
doi:10.1088/1367-2630/11/1/013015

Charge dependence of nano-particle growth in silane plasmas under UV irradiation

C R Seon[1,3], W Choe[1,4], K B Chai[1], H Y Park[1] and S Park[2]

[1] Department of Physics, Korea Advanced Institute of Science and Technology, 335 Gwahangno, Yuseong-gu, Daejeon 305-701, Korea
[2] Korea Research Institute of Standards and Science, 1 Doryong-dong, Yuseong-gu, Daejeon 305-340, Korea

[3] Present address: National Fusion Research Institute, 113 Gwahangno, Yuseong-gu, Daejeon 305-333, Korea.

[4] Author to whom any correspondence should be addressed.

E-mail: wchoe@kaist.ac.kr

Received 27 September 2008
Published 7 January 2009

Abstract. The controlled generation of nano-particles has been an important issue for the nano-structure formation in processing plasmas. We observed that the particle growth under UV irradiation was enhanced due to electric charge reduction of the particles, suggesting that the variation of particle charges could be a control parameter for the particle growth. The particle growth variation by UV irradiation is well described by the particle coagulation model with time-dependent particle charges in consideration, where predator particles grow by adsorbing a few nanometer-sized proto-particles.

Contents

1. Introduction

Particles are often generated in gas-phase during plasma-aided processes such as plasma enhanced chemical vapor deposition (PECVD) and reactive ion etching (RIE), and they can be detrimental or beneficial depending on application. In the semiconductor industries, the particles are known to be responsible for yield loss because of wafer contamination by fallen particles. The removal of the particles out of the plasma processing ambient has become more important as the feature size of the integrated circuit rapidly decreases. In other aspects, the inclusion of nano crystalline silicon particles in amorphous hydrogenated silicon (a-Si : H) films results in a photovoltaic cell with better electronic properties and enhanced stability against light-induced defect creation [1]. The replacement of the poly-disperse silicon floating gate structure with nanometer-sized mono-disperse silicon particles was also suggested in the development of the next generation flash-gate memory [2]. Furthermore, the visible emission from the quantum confined Si nano-particles was observed, and the electro-luminescent display with Si nano-particles has been actively studied [3, 4].

For both removal and innovative utilization of particles, the controlled generation of particles has been under active research. For example, it was reported that the particle growth is affected by variation of the discharge frequency [5]. By increasing the discharge frequency, particles appeared at earlier discharge time, but the size growth rate in the subsequent phase decreased. In [6], the sequential operation of capacitive and inductive discharge modes was used to control the particle size.

In addition to the aforementioned methods, the electric charge of particles can be an effective control knob for generation and removal of the particles in plasmas because the particle coagulation might be affected by the electric charge of the particles. The particle charge could be varied by UV irradiation [7]–[10]. The experimental studies on UV–particle interaction so far have focused on the photoelectric charging of macroscopic particles injected intentionally from outside the plasmas, and the effect of UV irradiation on growing particles was studied only in the numerical calculation [7]. In the present paper, we report the experimental results of the role of UV on nano-particle growth in silane plasmas. The speed-up of the particle growth was observed as UV irradiated the particles.

In the particle coagulation model of [7], some of the initial particles (about 2 nm) have positive charges by UV irradiation, and the coagulation between oppositely charged initial particles enhanced. However, in the present paper, the particle coagulation model is modified by assuming that all initial particles have negative charges, and the coagulation under UV irradiation is enhanced due to the reduced repulsive forces between the particles by reduced negative charges. The measured particle growth was in good agreement with the modified coagulation model.

2. Experimental setup

A schematic diagram of the experimental setup is presented in figure 1. Experiments were carried out using a 13.56 MHz capacitively-coupled plasma reactor at 50–70 W radio-frequency (rf) power and 5%SiH_4 gas diluted by 95% Ar at 30–80 m Torr pressure. The laser light scattering (LLS) diagnostic employing a 30 mW continuous-wave He–Ne laser was used for particle size measurement. A charge-coupled device (CCD) camera with imaging optics was used to measure the scattering light intensity, and a 632.8 nm filter was positioned in front of the camera to remove the unwanted light coming from the plasma. The size measurement was performed at the radial center of the electrode and 19 mm above the bottom powered electrode where the generated particles were levitated. Electron density and temperature were measured using a floating-type probe at the same position where the size measurement was performed.

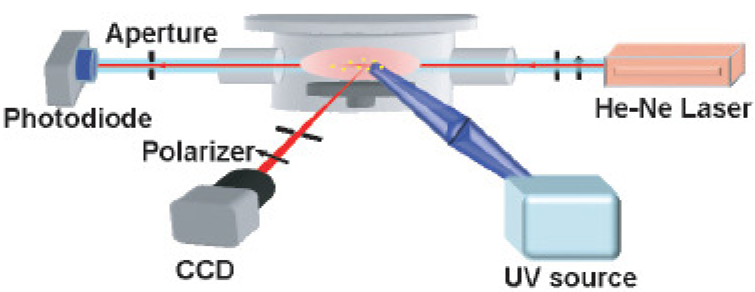

Figure 1. A schematic diagram of the experimental arrangement.

The UV light source (Hoya-Schott EX250) provided an irradiation power of 406 mW cm^{-2} in the wavelength range of $\lambda = 240$–450 nm. The initial illumination area was focused to about 2 cm×2 cm at 32 cm away from the source after passing through the collimation optics. The vertical center of the irradiation coincided with the position where all the measurements were performed ($z = 19$ mm). Based on the work function of 4.07 eV (or $\lambda = 305$ nm) of Si : H particles which corresponds to the electron affinity of bulk silicon [7], the UV irradiation power of $\lambda < 305$ nm for inducing photoemission from Si : H particles is estimated to be about 80 mW cm^{-2}. It was experimentally confirmed by optical emission spectroscopy and a floating probe that the used UV power level did not bring about any significant change in the plasma properties.

3. Results and discussions

Figure 2(a) shows the measured particle size with and without the UV irradiation at 80 m Torr and 70 W. The temporal pattern of the particle growth is a sequence of fast coagulation, slow growth, and saturation and/or strong particle transport due to large particle size, as illustrated in the figure [11]–[13]. The measurement over a longer time showed a new growth cycle with the same temporal pattern. As UV photons are irradiated on the particles, the fast growth phase appears about 10 s earlier and the particle growth rate is higher compared to the case without the UV irradiation. Subsequently, the particles grow up to about 90 nm in diameter before the growth saturates. In comparison, the saturated diameter is about 80 nm in the absence of the UV irradiation.

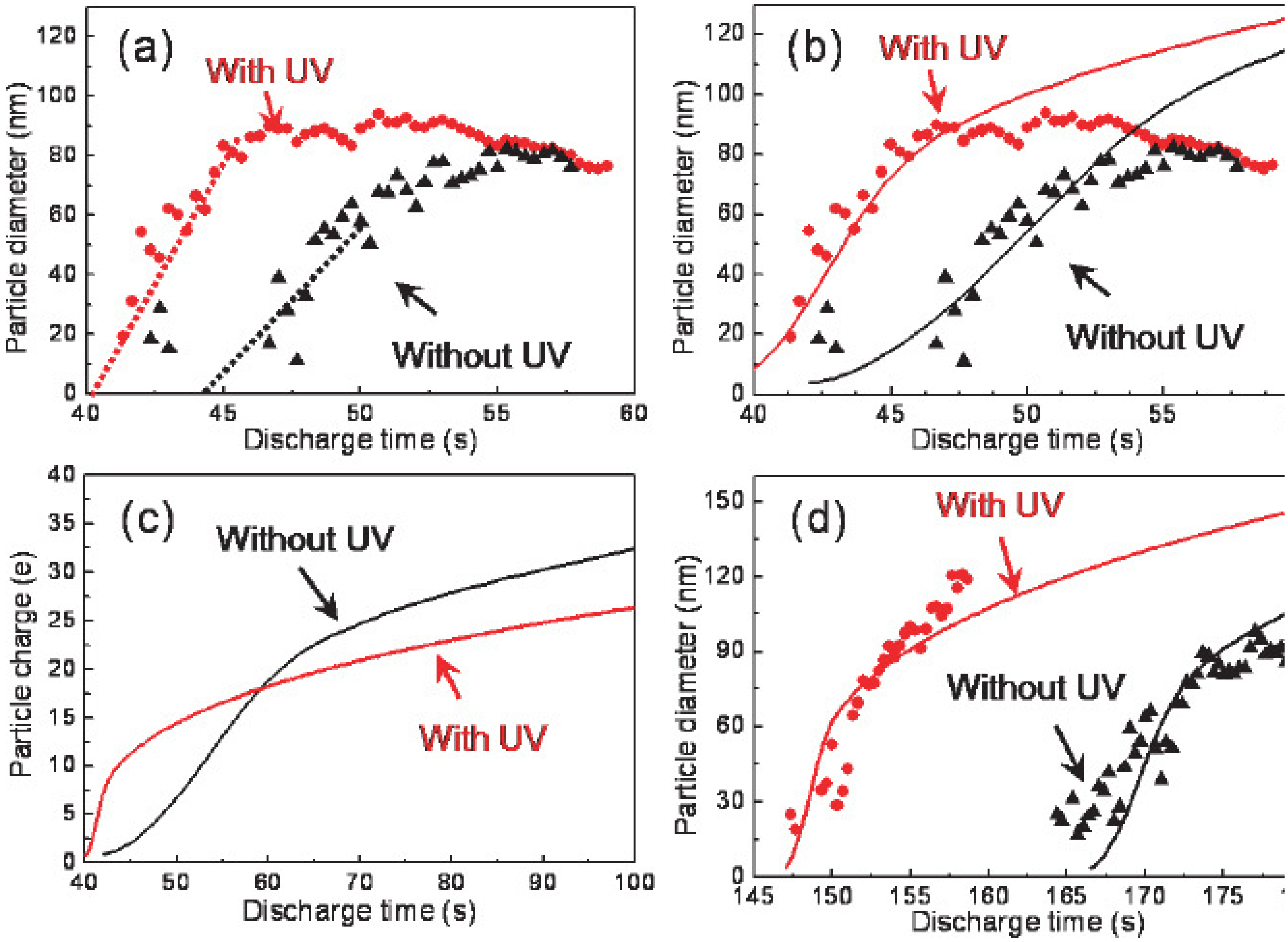

Figure 2. (a) The measured particle sizes at 19 mm above the electrode at 80 m Torr and 70 W. The circles (triangles) correspond to the case with UV irradiation (without UV irradiation). (b) The particle size by measurement and that by modeling are compared. (c) The temporal change of the particle charges obtained from the modeling. (d) The particle size by measurement and that by modeling at 32 m Torr and 50 W.

In the same manner, the measurement was repeated for the 32 m Torr and 50 W discharge. Figure 2(d) demonstrates the measured size after the start of a new particle growth cycle. The temporal pattern of the particle growth appears about 20 s earlier in the UV irradiation case. By comparing figures 2(a) and (d), it is found that the irradiation of UV is more effective on the particle growth at 32 m Torr and 50 W, i.e. at lower rf power and pressure.

The enhancement of particle growth by UV irradiation is confirmed by scanning electron microscopy (SEM) photographs of the particles shown in figure 3. The photographs were obtained under the same discharge condition of 32 m Torr, 50 W at 150 s after the plasma onset. Note that particles grow up to about 80 nm in diameter under the UV irradiation, which is about ten times larger than the case in the absence of the UV irradiation. The sizes in figure 3 are consistent with the sizes from the LLS diagnostic shown in figure 2(d).

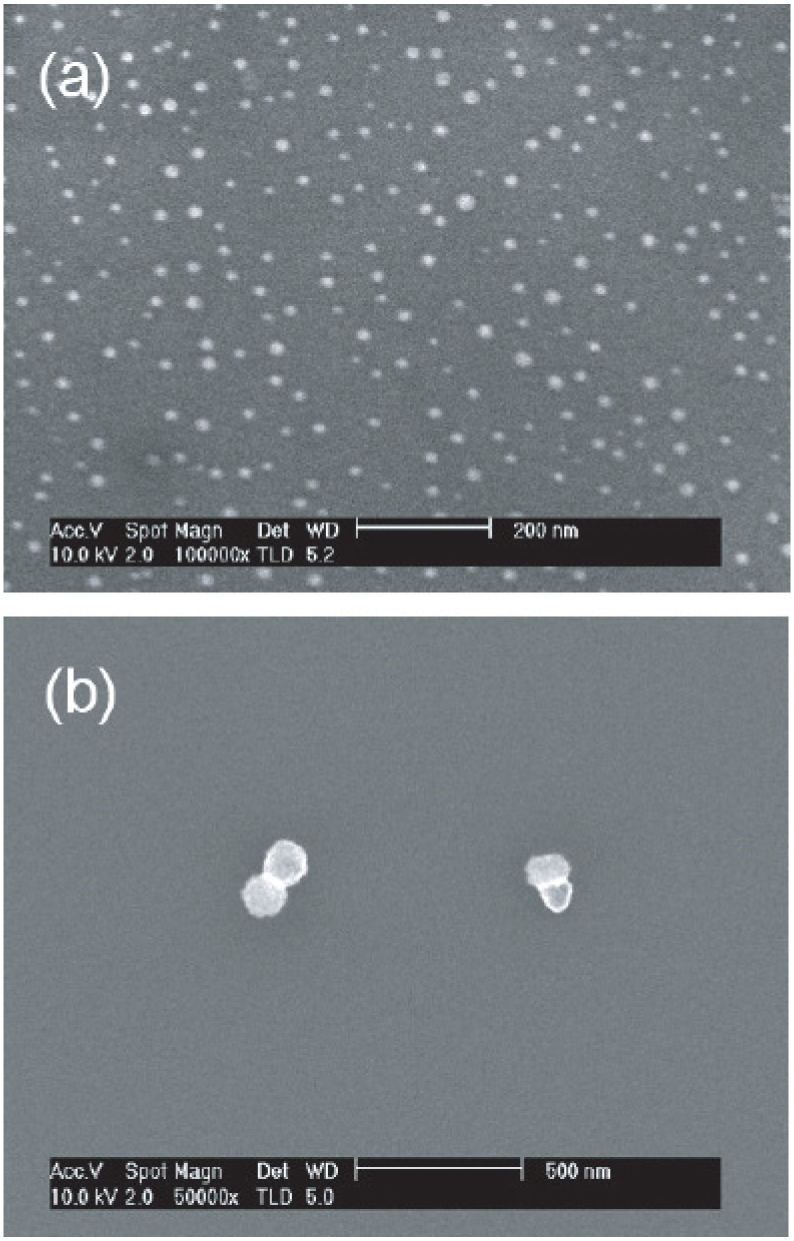

Figure 3. The scanning electron microscopy photographs collected in the 32 m Torr and 50 W discharge at 150 s: (a) without UV irradiation and (b) with UV irradiation.

The drastic enhancement of the particle growth is attributed to the change of particle charge caused by UV photons. As the irradiated UV photons induce photoemission from the particles, the particle charges become less negative. This reduces the repulsive force between the particles, which causes more active particle coagulation. Further understanding of the particle growth in the presence of UV irradiation was attempted by the particle coagulation modeling suggested by Lemons and Keinigs [14] with modification. Without taking particle transport into account, it is assumed that predator particles of radius R grow by coagulation of several nm-sized proto (prey) particles of radius R_0. The temporal change of the mass M of a predator particle can be described as

$$\frac{\mathrm{d}M}{\mathrm{d}t} = \rho\beta(R,\, R_0), \qquad (1)$$

where $\rho = \rho(t)$ is the time-dependent proto-particle mass density, and $\beta(R,R_0)$ is the coagulation rate including particle charges, which are functions of $R(t)$ and $R_0(t)$. On the other hand, the coagulation rate $\beta(R,R_0)$ is described as [7]

$$\beta(R, R_0) = \exp\left[-\frac{Z(R)Z(R_0)e^2}{4\pi\varepsilon_0(R+R_0)kT_d}\right]\left(\frac{4\pi}{3}\right)^{5/6}\left(\frac{6kT_d}{\rho_d}\right)^{1/2}\left(\frac{1}{R^3}+\frac{1}{R_0^3}\right)^{1/2}(R+R_0)^2,$$

where $Z(R)e$ and $Z(R_0)e$ are electric charges of predator and proto particles of radius R and R_0, respectively, and ρ_d is the mass density of a single particle. In equation (2), the exponential term is from the OML theory [15]. Note that the charges of both particles have the same polarity. Other terms describe dependences of the coagulation rate on thermal speed and particle size.

By using equation (1) and following the procedure in [14], the temporal evolution of the particle radius is described by

$$\frac{dR}{dt} = \frac{\beta(R, R_0)}{4\pi\rho_d R^2}\left[n_g m_0 + \rho_0' t - n_g m_0\left(\frac{R}{R_0}\right)^3\right], \tag{3}$$

where n_g is the constant predator particle number density, ρ_0' is the constant creation rate of the proto particle mass density and $m_0 = 4\pi\rho_d R_0^3/3$. The last term of the above equation is related to the mass density loss due to adsorption to the predator particles.

The particle charge $Z(R)e$ is calculated by balancing the electron current and the ion current flowing into the particle and the photo emission current, i.e. $I_e = I_i + I_{ph}$ because the particle charge is determined by charge neutrality condition. The electron current I_e and the ion current I_i are expressed as [15]

$$I_e = \pi R^2 n_e e\sqrt{\frac{8kT_e}{\pi m_e}}\exp\left(-\frac{Ze^2/4\pi\varepsilon_0 R - e\Phi_p}{k_B T_e}\right), \tag{4}$$

$$I_i = \pi R^2 n_i e\sqrt{\frac{8kT_i}{\pi m_i}}\left\{1+\frac{2\pi(Ze^2/4\pi\varepsilon_0 R - e\Phi_p)}{8k_B T_i}\right\}, \tag{5}$$

where T_e, T_i and Φ_p are electron temperature, ion temperature and plasma potential, respectively. As the particles are negatively charged, the photoemission current is given as [9]

$$I_{ph} = \pi R^2 e J Q_{abs} Y, \tag{6}$$

where J is the incident UV photon flux, Q_{abs} is the absorption efficiency of the photons and Y is the photoelectric efficiency.

The charge calculation was performed for the 80 m Torr and 70 W discharge. Under the condition, the electron temperature and density were measured to be $k_B T_e = 10$ eV and $n_e = 5\times10^9$ cm^{-3} at the radial center and 19 mm above the electrode, and we use the measured values in the modeling. The ions and particles are assumed to be at room temperature, i.e. $k_B T_i = 1/40$ eV and $k_B T_d = 1/40$ eV. In the pre-sheath region where the size measurement was performed, the electrostatic potential is set to be a certain value between the plasma potential and the sheath boundary potential ($\simeq -kT_e/2$) so that $\Phi_p = -1.52$ V is taken. For the efficiency, $Q_{abs} = 0.1$ and $Y = 0.02$ are assumed because dielectric particles such as amorphous silicon have values of $Y \simeq 0.01$–0.1 and $Q_{abs} \leq 1$ at $2\pi R/\lambda \geq 1$, where R and λ are the particle radius and UV wavelength, respectively [7, 9, 10]. From $I_e = I_i + I_{ph}$, the particle charge $Z(R)e$ is calculated as a function of particle radius R. In the case without UV irradiation ($J = 0$ mW cm^{-2}), $Z(R) = 0.243\ R$ (with R in nm) is obtained, and in the case with UV irradiation ($J = 80$ mW cm^{-2}), $Z(R) = 0.194\ R$.

Having the calculated particle charges $Z(R)e$ and $\beta\ (R,R_0)$ from equation (2), equation (3) is solved using the proto particle radius $R_0 = 1.3$ nm and the predator particle density $n_d = 6.8 \times 10^{13}$ m^{-3} based on [8]. The calculated results (curves) are compared with the measured particle sizes at 80 m Torr and 70 W, as shown in figure 2(b), in which the modeling reasonably well describes the growth of the particle size for both with and without UV irradiation cases. The difference at the later times is due to the particle transport as the particle size becomes large enough, causing the particles dragged out of the measurement region by the ion drag force. Here, the time evolution of particle charges from the modeling is also depicted in figure 2(c). Because the particle charge is dependent on the particle size, the particle charge with the UV irradiation is larger than that without the UV from 40 s to 60 s. Since the particle growth is saturated after 60 s as shown in the modeling, the particle charge with the UV irradiation appears to be smaller than that without the UV due to the photoemission from the particles, as expected.

In the same manner, the calculation was repeated for the 32 m Torr and 50 W discharge, and the result is shown as curves in figure 2(d). In this case, $k_BT_e = 5$ eV, $n_e = 3 \times 10^9$ cm^{-3}, $k_BT_i = 1/40$ eV, $k_BT_d = 1/40$ eV, and $\Phi_p = -1.70$ V are used. Again, reasonably good agreement is seen between the modeling and the experimental results.

To confirm the particle charge variation induced by UV, an experiment was performed to measure the change in particle levitation positions when the UV irradiation was abruptly turned on. The negatively-charged particles levitate around the sheath or pre-sheath region where the net force exerted on each particle vanishes. Figure 4(a) shows the image from the CCD camera while the UV irradiation was turned off. It is found that the levitation position shifts toward the lower electrode immediately after the UV light is turned on, as depicted in figure 4(b). The result of the image analysis of the pictures indicates that the displacement of the particle levitation is about 0.2 mm (figure 4(c)). Since the electrostatic force pointing upward is proportional to the particle charge, the downward shift of the levitation position indicates the reduction of the particle charge.

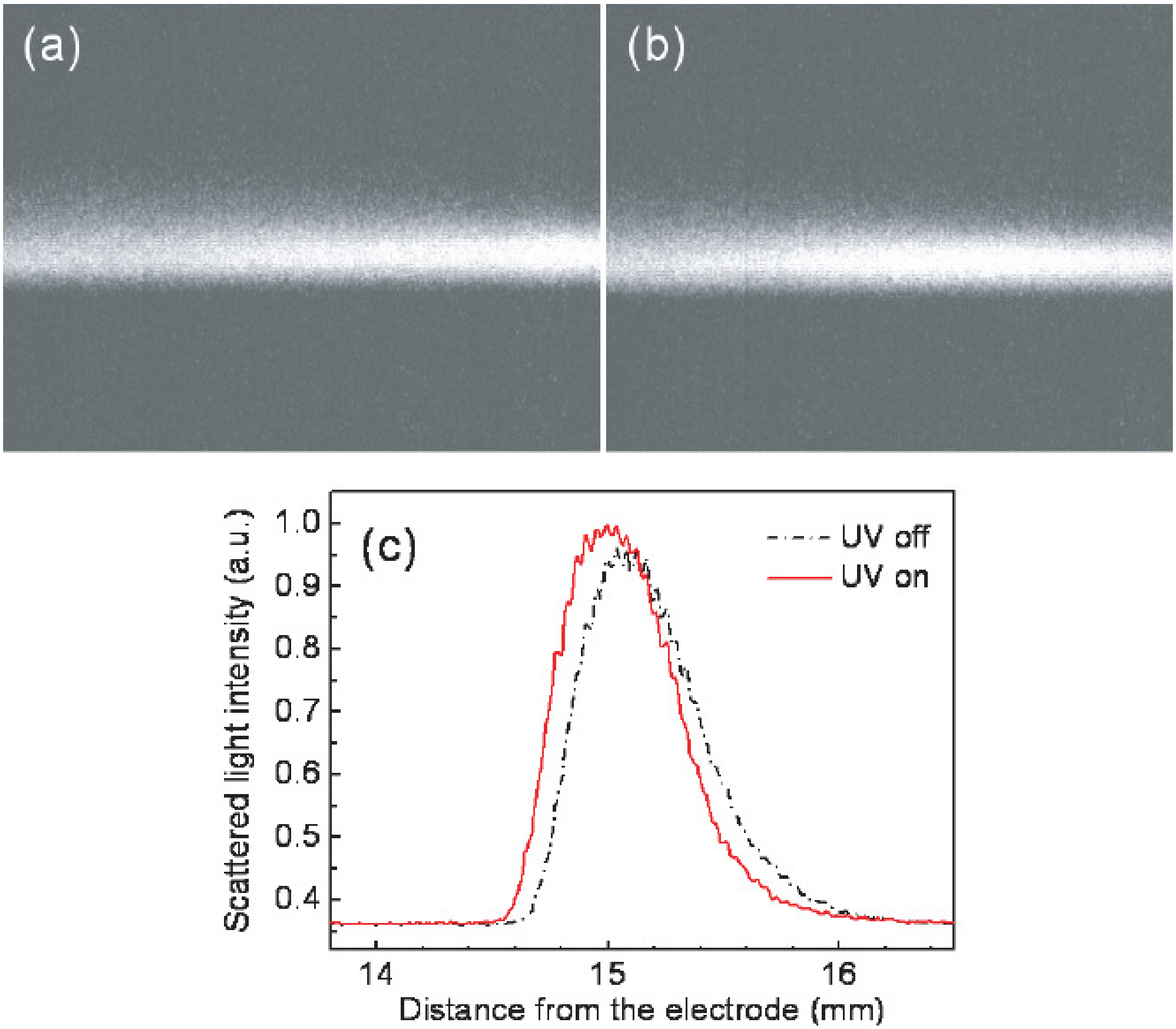

Figure 4. (a) The CCD image of the scattered light at 140 s in the 32 m Torr and 50 W discharge while UV irradiation is turned off. (b) The image at 141 s with the UV irradiation turned on. (c) The comparison in the scattered light intensity profile as a function of the distance from the lower electrode, showing the particle levitation position shifted toward the lower electrode with the UV irradiation turned on.

4. Conclusions

It is observed that the particle growth is enhanced in the presence of UV irradiation on Si : H particles, and the maximum particle size measured at the same location inside the plasma is also larger under the UV irradiation. The temporal evolution of the particle growth is well described by the modified coagulation model with consideration of time-dependent particle charge. The photoemission from the particle due to the UV irradiation reduces the particle charge, which is confirmed experimentally by the downward displacement of the particle levitation. As a result of the reduced charge, the reduction of repulsive force between the particles is the main cause of the growth enhancement or the increase of the coagulation rate. The results imply that the particle charge variation may become an effective control for the particle growth. It is noteworthy that UV irradiation is more effective on particle growth at lower rf power and gas pressure, because the photo-emission from dust particles is relatively more significant in the low electron current to dust particles.

Acknowledgments

This work was supported by the Korea Research Foundation grant funded by the Korean Government (KRF-2008-314-C00085).

References

[1] Thompson S, Perrey C R, Carter C B, Belich T J, Kakalios J and Kortshagen U 2005 *J. Appl. Phys.* **97** 034310
CrossRef Link | Order from Infotrieve

[2] Tiwari S, Rana F, Hanafi H, Hartstein A, Crabbé E F and Chan K 1996 *Appl. Phys. Lett.* **68** 1377
CrossRef Link | Order from Infotrieve

[3] Ligman R K, Mangolini L, Kortshagen U R and Campbell S A 2007 *Appl. Phys. Lett.* **90** 061116
CrossRef Link | Order from Infotrieve

[4] Photopoulos P and Nassipolulou A 2000 *Appl. Phys. Lett.* **77** 1816
CrossRef Link | Order from Infotrieve

[5] Watanabe Y, Shiratani M, Fukuzawa T, Kawasaki H, Ueda Y, Singh S and Ohkura H 1996 *J. Vac. Sci. Technol.* A **14** 995
CrossRef Link | Order from Infotrieve

[6] Schulze M, von Keudell A and Awakowicz P 2006 *Appl. Phys. Lett.* **88** 141503
CrossRef Link | Order from Infotrieve

[7] Kortshagen U and Bhandarkar U 1999 *Phys. Rev.* E **60** 887
CrossRef Link | Order from Infotrieve

[8] Sickafoose A A, Colwell J E, Horanyi M and Robertson S 2000 *Phys. Rev. Lett.* **84** 6034
CrossRef Link | PubMed Abstract | Order from Infotrieve

[9] Samarian A A, Vaulina O S, Nefedov A P, Fortov V E, James B W and Petrov O F 2001 *Phys. Rev.* E **64** 056407
CrossRef Link | Order from Infotrieve

[10] Rosenberg M, Mendis D A and Sheehan D P 1996 *IEEE Trans. Plasma Sci.* **24** 1422
CrossRef Link | Order from Infotrieve

[11] Hollenstein Ch, Dorier J-L, Dutta J, Sansonnens L and Howling A A 1994 *Plasma Sources Sci. Technol.* **3** 278
IOP Article

[12] Boufendi L, Hermann J, Bouchoule A, Dubreuil B, Stoffels E, Stoffels W W and Giorgi M L 1994 *J. Appl. Phys.* **76** 148
CrossRef Link | Order from Infotrieve

[13] Samsonov D and Goree J 1999 *J. Vac. Sci. Technol.* A **17** 2835
CrossRef Link | Order from Infotrieve

[14] Lemons D S and Keinigs R K 1996 *Appl. Phys. Lett.* **68** 613
CrossRef Link | Order from Infotrieve

[15] Shukla P K and Mamun A A 2002 *Introduction to Dusty Plasma Physics* (Bristol: Institute of Physics Publishing) pp 36–47